DETERMINING THE COMPOSITION OF VARIOUS MARTIAN CENTRAL MOUNDS. A. C. Pascuzzo[1], J. F. Mustard, [1]Dept. of Earth, Environmental, and Planetary Sciences, Brown University, Providence, RI, 02912 (alyssa_pascuzzo@brown.edu)

Introduction: Martian craters containing central mound sedimentary deposits has been a curious topic of debate for many years [1-8]. A central mound can be loosely defined as a rounded interior crater deposit with substantial thickness relative to the crater floor (some with mound heights exceeding that of the crater rim) [1]. Many, but not all, have a moat around the perimeter of the mound and the crater wall [1]. Proposed mechanisms for central mound formation include lacustrine, deltaic, alluvial, aeolian, explosive volcanism, impact-related, and ice-related processes [1-8]. Without a comprehensive comparative study of mound composition with varying mound morphology and location makes ground truthing mound formation processes quite challenging.

A recent global survey of martian craters identified 50 craters (within ±60° latitude, >25 km in diameter, mound height >20% of crater floor to rim height) containing a central mound deposit [4]. The majority of central mounds are located in and around Arabia Terra (Fig. 1). Others are found near the Medusae Fossae Formation (MMF), Hellas and Argyre Basins [4]. Included in the list of the 50 central mounds is Mt. Sharp, in Gale crater. Mt. Sharp is one of the thickest mounds known, rising higher than its host crater's rims by hundreds of meters with a mound thickness of ~5 km. The lowest units of Gale's mound are currently being investigated by the *Curiosity* rover. Both CRISM and *Curiosity* detected phyllosilicates and hydrated sulfates in the lower portions of Mt. Sharp, thus supporting aqueous processes being responsible for a large portion of Mt. Sharp's formation.

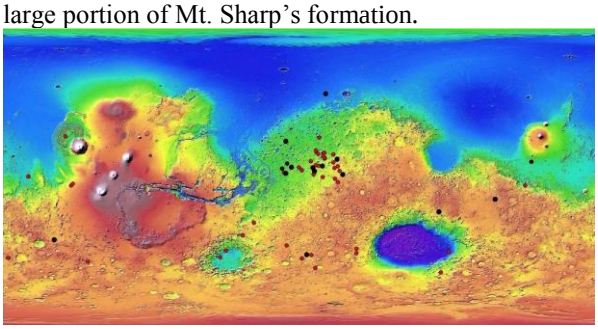

Figure 1. *Distribution of the initial 50 central mound craters [4] plus the added 9 from this study (red markers) compared to the distribution of the 16 central mound craters (black markers) that have minimal dust coverage, high thermal inertia and contain CRISM images with promising spectral signatures, mapped on MOLA basemap*

Mt. Sharp is the most understood central mound in terms of composition and formation history. However, how does our understanding of Mt. Sharp relate to central mounds as a whole? The formation and evolu tion of central mounds and their relationship to one another on a global scale is controversial, but enquiries of various central mounds with high spatial and spectral analyses of Compact Reconnaissance Imaging Spectrometer for Mars (CRISM) [9] data will help clarify such uncertainties regarding composition.

Method for Central Mound Selection: An additional 9 craters where added to the initial 50 craters identified previously [4] for a larger sample size. Out of the 59 craters (Fig. 1), 31 have CRISM footprint coverage of the host crater – not limited to coverage of the host's mound. CRISM data (1-2.6μm) was processed using the CRISM Analysis Tools (CAT) in ENVI, including atmospheric, photometric, and destriping corrections. The available, 103, CRISM images of the craters were cross-referenced with the TES dust cover map [10] and THEMIS nighttime infrared images [11] for exposed or cemented bedrock. Craters and mounds with minimal dust coverage and high thermal inertias were selected as promising candidates for further analyses. All 103 images were briefly analyzed in ENVI to avoid omitting CRISM images that may initially appear unpromising from the TES dust cover data and THEMIS nighttime infrared images.

Table 1. *Central mound craters being analyzed in this study.* (*) *Mound height data from Bennett & Bell (2016)*

Latitude, Longitude	Diameter (km)	Crater name	Mound Height (m)
-46.99, 4.90	79	Asimov	2000
-38.11, -149.05	83		1860*
-21.19, 85.11	113	Millochau	375
-13.59, 119.64	44	-	1014*
1.57, 26.72	96	-	2317*
2.15, -7.83	52	-	687*
3.67, 9.63	27	-	800
5.08, -10.14	110	Crommelin	2171*
5.61, 8.59	58	-	1313*
5.90, -4.44	56	Vernal	710*
6.59, 14.31	69	Capen	771*
7.98, -7.05	64	Danielson	1974*
8.93, 141.28	51	-	1306*
10.79, 23.45	168	Henry	2040*
21.89, -7.94	165	Becquerel	1085*
50.56, 16.35	50	Micoud	951*

Initial Spectral Analyses Results: A total of 26 CRISM images from 16 craters (Fig. 1, Table 1) displayed variation in reflectance spectra properties that may correspond to distinct mineralogic signatures on or around the central mound.

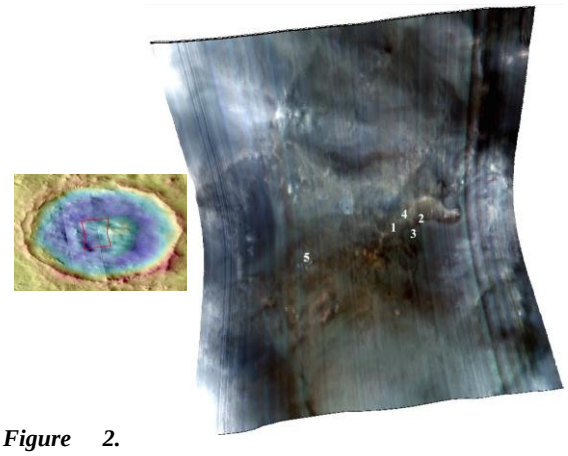

Figure 2. *Micoud crater CRISM false color image FRT00019658. Numbered locations correspond to spectra in Fig. 3.*

Micoud Crater. FRT00019658 (Fig. 2) covers the western half of the mound in Micoud - the northern most crater of the dozen. Micoud's mound surrounds a central uplift peak, however, distinction between the mound and central peak is difficult. The chaotic and intermittent terrain of the mound is unique compared to the majority of central mounds. Spectra (5x5 pixels) were taken from areas that appeared green in the false color image. Spectra from these locations where analyzed by dividing the spectra of interest by a spectrally 'bland' region (5x5 pixels) from the same column (Fig. 3a).

The spectral features of the ratioed spectra are similar to those of library spectra of chlorite and illite (Fig. 3b). However, the spectra do not exhibit a 1.4µm H_2O/OH vibrational feature as expected. The five ratioed spectra have a weak 1.9µm H_2O band, although the strength varies between spectra. Spectra 2 and 3 have 2.23 and 2.35µm bands similar in strength to each other, diagnostic of illite. Spectra 1, 4, and 5 have a strong 2.35µm band in addition to a weaker 2.24µm feature. The 2.24µm feature is broader than expected for chlorite, which could be due to mixing of hydrated mineral phases.

Areas with moderate to strong detections of Fe/Mg phyllosilicates are sparse and appear on various slopes of the mound in this image. Surrounding areas, spatially close to Fe/Mg phyllosilicates shown as red-brown in the figure 2, are dominated by strong olivine and pyroxene signatures and minimal to zero indications of Fe/Mg phyllosilicates. Chlorite-illite mineral assemblage suggests hydrothermal alteration of olivine, however, prehnite was not detected[12].

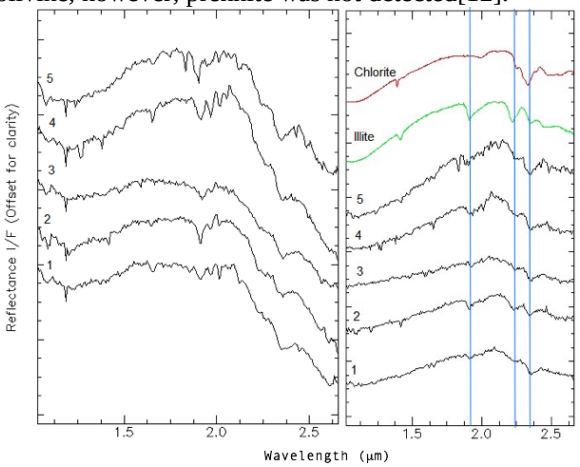

Figure 3. *(a) I/F reflectance spectra. 1-5 correspond to locations in figure 2. (b) Ratioed spectra (1-5) and library spectra of chlorite and illite. Vertical blue lines point to the absorption features in the spectra at 1.9, 2.23-2.24, & 2.35 µm. Spectra are offset for clarity.*

Conclusions and Further Work: Formation of Micoud's central mound is likely the product of reworking and weathering of the crater's central peak material, however, distinguishing between the mound and the central uplift needs further analyses. The initial impact responsible for the crater would have generated heat, which could have melted any surface/subsurface ice and/or excavated buried hydrated mineral bearing units [13]. This suggests the primary mechanisms responsible for Micoud's mound formation are a combination of impact-related processes and various forms of erosion and weathering.

Ongoing CRISM analyses of the 16 central mound craters will continue in addition to mineral and morphologic mapping for all 16 mounds to further determine the mineralogy and possible origin of the various mounds.

References: [1] Malin & Edgett (2000) *Science, 290*, 1927-1937 [2] Thomson et al. (2011) *Icarus, 214*, 413-432 [3] Andrews-Hanna et al. (2010) *JGR*, 115, E06002 [4] Bennett & Bell (2016) *Icarus, 264*, 331-341 [5] Kite et al. (2013) *Geo., 41*, 543-546 [6] Cabrol & Grin (1999) *Icarus, 142 (1)*, 160-172 [7] Fergason & Christensen (2008) *JGR, 113 (E12)* E12001 [8] Rossi et al. (2008) *JGR, 113 (E8)*, E08016 [9] Murchie et al. (2007) *JGR, 116*, E10008 [10] Ruff & Christensen (2002) *JGR, 107*, E001580 [11] Edwards et al. (2011) JGR, 116, E10008 [12] Ehlmann et al. (2011) *Clays & Clay Min., 59 (4)*, 359-377 [13] Sun & Milliken (2015) *JGR, 120*, E004918